

Extremely strong C IV $\lambda 1550$ nebular emission in the extremely low-metallicity star-forming galaxy J2229+2725

Y. I. Izotov^{1*}, D. Schaerer^{2,3}, N. G. Guseva¹, T. X. Thuan⁴ and G. Worseck⁵

¹*Bogolyubov Institute for Theoretical Physics, National Academy of Sciences of Ukraine, 14-b Metrolohichna str., Kyiv, 03143, Ukraine,*

²*Observatoire de Genève, Université de Genève, 51 Ch. des Maillettes, 1290, Versoix, Switzerland,*

³*IRAP/CNRS, 14, Av. E. Belin, 31400 Toulouse, France,*

⁴*Astronomy Department, University of Virginia, P.O. Box 400325, Charlottesville, VA 22904-4325,*

⁵*Institut für Physik und Astronomie, Universität Potsdam, Karl-Liebknecht-Str. 24/25, D-14476 Potsdam, Germany*

6 November 2023

ABSTRACT

Using *Hubble Space Telescope* (*HST*)/Cosmic Origins Spectrograph (COS) observations of one of the most metal-poor dwarf star-forming galaxies (SFG) in the local Universe, J2229+2725, we have discovered an extremely strong nebular C IV $\lambda 1549$, $\lambda 1551$ emission-line doublet, with an equivalent width of 43\AA , several times higher than the value observed so far in low-redshift SFGs. Together with other extreme characteristics obtained from optical spectroscopy (oxygen abundance $12 + \log(\text{O}/\text{H}) = 7.085 \pm 0.031$, ratio $\text{O}_{32} = I([\text{O III}]\lambda 5007)/I([\text{O II}]\lambda 3727) \sim 53$, and equivalent width of the $\text{H}\beta$ emission line $\text{EW}(\text{H}\beta) = 577\text{\AA}$), this galaxy greatly increases the range of physical properties for dwarf SFGs at low redshift and is a likely analogue of the high-redshift dwarf SFGs responsible for the reionization of the Universe. We find the ionizing radiation in J2229+2725 to be stellar in origin and the high $\text{EW}(\text{C IV } \lambda 1549, 1551)$ to be due to both extreme ionization conditions and a high carbon abundance, with a corresponding $\log \text{C}/\text{O} = -0.38$, that is ~ 0.4 dex higher than the average value for nearby low-metallicity SFGs.

Key words: galaxies: dwarf – galaxies: starburst – galaxies: ISM – galaxies: abundances.

1 INTRODUCTION

In a scenario of hierarchical structure formation and during the epoch of the reionization of the Universe, the majority of galaxies are expected to be of low-mass, strongly star-forming, and highly deficient in metals (e.g. Mascia et al. 2023). The low metallicity stellar populations in these galaxies with spectra steeply rising toward shorter wavelengths imply strong and possibly hard ionizing radiation, resulting in some cases in the presence of nebular emission of high-ionization species such as the C IV $\lambda 1549$, $\lambda 1551$ doublet (hereafter C IV $\lambda 1550$) in the UV range (e.g. Senchyna et al. 2017; Berg et al. 2019). Furthermore, these galaxies likely dominate the ionizing background at $z > 6$, and are thus probably the main sources of cosmic reionization, according to both recent observational evidence from their local analogues (Izotov et al. 2016a,b, 2018b,c, 2021b, 2022; Flury et al. 2022) and state-of-the-art numerical simulations (e.g. Rosdahl et al. 2018; Katz et al. 2021; Kannan et al. 2022). However, the detection of these high-redshift galaxies

is a difficult task because of their low mass and hence their extreme faintness. Only recently Atek et al. (2023), using *James Webb Space Telescope* (*JWST*) spectroscopic observations, have found $z \sim 6 - 7$ galaxies with stellar masses and metallicities as low as those in the most metal-deficient galaxies at low redshift. However detailed studies of these far-away objects remain difficult.

On the other hand, extensive searches for extremely metal-deficient galaxies (XMDs) at low-redshift have revealed star-forming galaxies (SFR) with masses down to $M_\star \sim 10^6 M_\odot$ and metallicities down to $12 + \log(\text{O}/\text{H}) \sim 7.0$ (e.g. Hirschauer et al. 2016; Hsyu et al. 2016, 2018; Senchyna & Stark 2019; Izotov et al. 2018a, 2019a, 2021a; Kojima et al. 2020). With these properties and showing very high star-formation activity (high specific star-formation rates, $\text{sSFR} \sim 100 - 300 \text{ Gyr}^{-1}$), these XMDs are likely the closest local analogues of dwarf galaxies in the early Universe. They represent unique laboratories to study the building blocks of galaxies in so-far unreachable detail.

Until recently, most of low- z metal-deficient galaxies were studied in the rest-frame optical range and very few UV spectra of them have been obtained. Be-

* Corresponding author: yizotov@bitp.kiev.ua

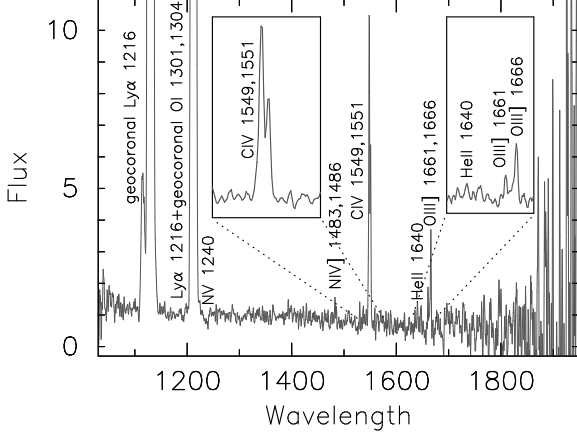


Figure 1. The restframe *HST*/COS spectrum of J2229+2727 with labelled lines. Fluxes are in units 10^{-16} erg s $^{-1}$ cm $^{-2}$ Å $^{-1}$ and wavelengths are in Å.

low $12 + \log(\text{O}/\text{H}) < 7.5$, only few low-redshift star-forming galaxies (SFG) have been observed with the *Hubble Space Telescope* (*HST*) so far (Berg et al. 2016, 2018, 2019; Senchyna et al. 2022). Recent searches have significantly expanded the samples of XMDs down to $12 + \log(\text{O}/\text{H}) \sim 7.0$, which now allow us to probe the least chemically-evolved SFGs and study their UV spectra. This permits to observe for the first time the main UV emission lines of such extreme galaxies, in the wavelength range between Ly α (1216Å) and ~ 1900 Å, and which include the C iv $\lambda 1550$ doublet, He ii $\lambda 1640$, O iii] $\lambda\lambda 1661, 1666$ (hereafter O iii] $\lambda 1663$), and possibly other lines.

In this paper we present *HST* observations of one of the most metal-deficient galaxies, J2229+2725, with $12 + \log(\text{O}/\text{H}) = 7.085$. Its properties from optical spectroscopic observations were studied in detail by Izotov et al. (2021a). Some of these properties are shown in Table 1. The most notable are an extremely high equivalent width EW(H β) of 577Å and an extremely high O $_{32}$ ratio of 53. Both characteristics indicate that the ionizing parameter and/or the hardness of ionizing radiation are considerably higher in J2229+2725 than in other star-forming galaxies.

2 THE UV SPECTRUM OF J2229+2725

HST/Cosmic Origins Spectrograph (COS) spectroscopy of J2229+2725 was obtained in program GO 17100 (PI: Y. I. Izotov) on 23 July 2023. The galaxy was acquired by COS near-ultraviolet (NUV) imaging. The spectrum with an exposure time of 12282 sec was obtained with the G140L grating. It was reduced with the CALCOS pipeline v3.3.4.

The UV spectrum of J2229+2725 is shown in Fig. 1. Its most striking feature is the very strong narrow C iv $\lambda 1550$ doublet, without any indication of the stellar absorption lines which are commonly seen in star-forming galaxies with higher metallicities. The weaker nebular lines N iv] $\lambda 1483, 1486$, He ii $\lambda 1640$, and O iii] $\lambda 1663$ doublet are also detected. We also note the presence of the stellar absorption line N v $\lambda 1240$, produced by massive stars with stellar winds. Unfortunately, the C iii] $\lambda 1909$ emission line

Table 1. Observed and derived characteristics of J2229+2725 †

Parameter	J2229+2725
R.A. (J2000)	22:29:33.19
Dec. (J2000)	+27:25:25.60
z	0.07622
M_g , mag	-16.39 ± 0.06
$\log L_g/L_{g,\odot}$	8.74
$\log M_*/M_\odot$	6.96
$L(\text{H}\beta)$, erg s $^{-1}$	$(3.1 \pm 0.3) \times 10^{40}$
EW(H β), Å	577 ± 4
SFR, M $_\odot$ yr $^{-1}$	0.68 ± 0.06
sSFR, Gyr $^{-1}$	75
O $_{32}$	53
$T_e(\text{O III})$, K	24800 ± 900
$N_e(\text{S II})$, cm $^{-3}$	1000 ± 600
$12 + \log \text{O}/\text{H}$	7.085 ± 0.031

† Data are taken from Izotov, Thuan & Guseva (2021a).

Table 2. Extinction-corrected line fluxes and equivalent widths in the UV spectrum of J2229+2725

Line	F^*	$100 \times I(\lambda)/I(\text{H}\beta)^\dagger$	EW ‡
N v $\lambda 1240$	-2.30 ± 0.40	-13.92 ± 2.91	-3.2 ± 0.7
N iv] $\lambda 1483$	0.61 ± 0.58	3.27 ± 3.12	1.1 ± 1.0
N iv] $\lambda 1486$	0.44 ± 0.58	2.38 ± 3.12	0.9 ± 1.1
C iv $\lambda 1549$	12.43 ± 1.22	66.81 ± 6.53	26.6 ± 2.7
C iv $\lambda 1551$	7.00 ± 1.21	37.63 ± 6.50	16.2 ± 2.8
He ii $\lambda 1640$	0.97 ± 0.45	5.15 ± 2.41	2.6 ± 1.2
O iii] $\lambda 1661$	1.29 ± 0.58	6.87 ± 3.12	3.3 ± 1.2
O iii] $\lambda 1666$	3.28 ± 0.58	17.46 ± 3.12	9.1 ± 1.2

* F is the observed flux in units of 10^{-16} erg s $^{-1}$ cm $^{-2}$.

$^\dagger I(\text{H}\beta) = 24.63 \times 10^{-16}$ erg s $^{-1}$ cm $^{-2}$ (Izotov et al. 2021a) and $I(\lambda)$ are extinction-corrected fluxes.

‡ Equivalent width in Å.

falls into the noisy part of the spectrum and therefore could not be seen.

In Fig. 2 we show the COS UV and Large Binocular Telescope (LBT) optical spectra of J2229+2725, superposed on the spectral energy distribution (SED) (black line) derived by Izotov et al. (2021a) from the LBT spectrum and extrapolated to the UV range. The SED consists of two components, nebular and stellar (blue and green lines, respectively). It is seen (as already noted by Izotov et al. 2021a) that the contribution of the nebular emission to the SED is high even in the UV range and dominates in the optical range. This is because of the extremely high EW(H β). The SED of the nebular continuum includes two-photon hydrogen emission and free-free and free-bound emission of hydrogen and helium (Aller 1984).

Nebular emission in the continuum of this galaxy is considerable even in the UV range longward of the Ly α line, due to sharply rising two-photon emission at $\lambda \geq 1215.67$ Å. Its contribution should be taken into account in the determination of stellar masses and of the UV stellar slope β , commonly used in studies of star-forming galaxies. Neglecting the nebular continuum contribution would make the stellar mass larger and the UV slope shallower.

We also note that the observed UV spectrum in Fig. 2 is in fair agreement with the extrapolated SED. However,

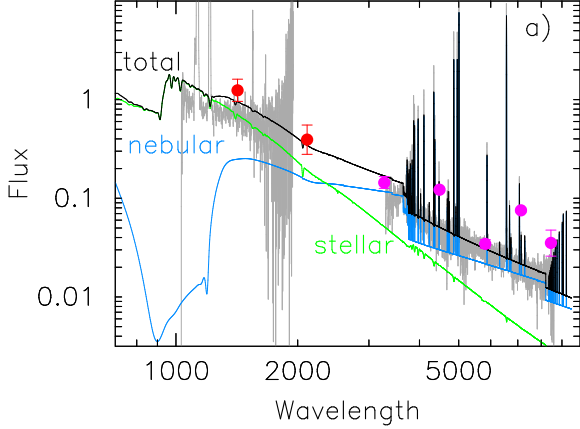


Figure 2. The SED obtained from fitting the rest-frame Large Binocular Telescope (LBT) spectrum taken from Izotov et al. (2021a). The observed UV and optical spectra are shown in grey, the modelled stellar, nebular, and total SEDs are shown by green, blue, and black lines, respectively, and are labelled. *GALEX* FUV, NUV, and SDSS *u, g, r, i,* and *z* photometric data, blueshifted adopting the J2229+2725 redshift, are shown by red and magenta filled circles, respectively. Fluxes are in units $10^{-16} \text{ erg s}^{-1} \text{ cm}^{-2} \text{ \AA}^{-1}$ and wavelengths are in \AA .

there is still some offset present. This offset can be caused by various reasons, for example, by uncertainties of SED fitting or possible vignetting of the COS spectrum.

We measure the line fluxes and equivalent widths in the observed UV spectrum and correct them for extinction, adopting $C(\text{H}\beta) = 0.060 \pm 0.038$ (Izotov et al. 2021a) and the reddening law of Cardelli, Clayton & Mathis (1989) with $R(V) = 2.7$. The results of the measurements are shown in Table 2.

3 ORIGIN OF STRONG NEBULAR C IV $\lambda 1550$ EMISSION

It is seen from Table 2 that the equivalent width of the C IV $\lambda 1550$ nebular emission doublet is extremely high, $\sim 43 \text{\AA}$. Such a high value is detected for the first time in the low-redshift and low-mass SFGs. However, it is similar to $\text{EW}(\text{C IV}) \sim 38 \text{\AA}$ found in the high- z galaxy A1703-zd6 at $z = 7.045$ (Stark et al. 2015). We also derive the high ionizing photon production efficiency $\xi_{\text{ion}} = 10^{25.92} \text{ Hz erg}^{-1}$, using the extinction-corrected $\text{H}\beta$ emission-line flux and the extinction-corrected flux of the COS spectrum at the rest-frame wavelength of 1500\AA (Fig. 2). These facts together with other extreme characteristics derived by Izotov et al. (2021a) make J2229+2725 an important marker, indicating the possible extended range of physical characteristics and tendencies in their relationships for galaxies with very young starbursts. The extremely high $\text{O}_{32} = 53$ of J2229+2725 corresponds to a very high ionization parameter $U \sim 10^{-1.7}$, according to Berg et al. (2019). This high U is due to an intense ionizing radiation, a young starburst age, corresponding to $\text{EW}(\text{H}\beta) = 577 \text{\AA}$, and a very compact structure of J2229+2725 (Izotov et al. 2024), with a high electron number density in its H II region $N_e([\text{S II}]) \sim 10^3 \text{ cm}^{-3}$ and $N_e([\text{Ar IV}]) \sim (3-4) \times 10^3 \text{ cm}^{-3}$ (Izotov et al. 2021a).

However, it is likely that the H II region is density-

bounded. This leads to a reduction of the O^+ zone and to an increase of O_{32} . Indeed, the double-peaked Ly α emission line is narrow in J2229+2725, with a small peak velocity separation of 207 km s^{-1} , corresponding to an escape fraction of ionizing LyC emission $f_{\text{esc}}(\text{LyC}) \sim 34$ per cent (Izotov et al. 2024).

We show in Fig. 3a the diagnostic diagram $I(\text{C IV } \lambda 1550)/I(\text{He II } \lambda 1640) - I(\text{O III] } \lambda 1663)/I(\text{He II } \lambda 1640)$ to constrain the origin of the ionizing radiation responsible for the strong C IV $\lambda 1550$ emission. J2229+2725 is located at the upper end of the distribution of low- and high- z SFGs, far from the location of AGN (shaded region), indicating that ionizing radiation in this galaxy producing C IV $\lambda 1550$ is stellar in origin. The absence of an AGN is to be expected for this galaxy as it is fully compatible with the optical line ratios, which clearly indicate stellar photoionization (see Izotov et al. 2021a).

In Fig. 3b, we show the relation between the C IV $\lambda 1550/\text{O III] } \lambda 1663$ flux ratio and the oxygen abundance $12 + \log(\text{O}/\text{H})$ for SFGs. This ratio in J2229+2725 (filled red circle) is considerably higher than those for SFGs from a comparison sample (blue and black filled circles). We consider two possible causes for this appearance: 1) a higher C/O abundance ratio compared to those in SFGs from the comparison sample and 2) higher ionization efficiency in this compact and dense galaxy, indicated by its extremely high O_{32} ratio, which is an observable characteristic of the high ionization parameter U , and very high ξ_{ion} . Both these effects may result in an increase of the C IV $\lambda 1550/\text{O III] } \lambda 1663$ flux ratio and of the equivalent width of C IV $\lambda 1550$ doublet in J2229+2725.

We adopt equation 4 of Pérez-Montero & Amorín (2017) and the electron temperature $T_e(\text{O III])} = 24800 \text{ K}$ (Table 1) for both the C^{3+} and O^{2+} species to derive the $\text{C}^{3+}/\text{O}^{2+}$ abundance ratio, using the extinction-corrected flux ratios of C IV $\lambda 1550$ and O III] $\lambda 1663$ (Table 2). We obtain $\log(\text{C}^{3+}/\text{O}^{2+}) = -0.76$.

The total C/O abundance is derived from Eq. 1, using the ionization correction factor $\text{ICF}(\text{C}^{3+}/\text{O}^{2+})$:

$$\frac{\text{C}}{\text{O}} = \frac{\text{C}^{3+}}{\text{O}^{2+}} \times \text{ICF} \left(\frac{\text{C}^{3+}}{\text{O}^{2+}} \right). \quad (1)$$

For the determination of $\text{ICF}(\text{C}^{3+}/\text{O}^{2+})$, we consider a set of the same photoionized H II region models calculated with the code CLOUDY (Ferland et al. 2013) as the ones used by Izotov et al. (2023a). However, here we select only models with an young age of 1 Myr, a high number density $N_e = 10^3 \text{ cm}^{-3}$ and $\text{O}_{32} > 10$. These parameters closely represent the physical conditions in J2229+2725 (Izotov et al. 2023a). The relation between $\text{ICF}(\text{C}^{3+}/\text{O}^{2+})$ and O_{32} in these models is shown in Fig. 4 and can be fit by the maximum likelihood linear regression

$$\text{ICF} \left(\frac{\text{C}^{3+}}{\text{O}^{2+}} \right) = 9.45 - 3.96 \times \log \text{O}_{32}. \quad (2)$$

We obtain $\text{ICF}(\text{C}^{3+}/\text{O}^{2+}) = 2.62$ (or $\log \text{ICF}(\text{C}^{3+}/\text{O}^{2+}) = 0.42$ dex), adopting the O_{32} value of 53 observed in J2229+2725. Finally, from Eq. 1 we derive $\log(\text{C}/\text{O}) = -0.38$. This $\log(\text{C}/\text{O})$ value is ~ 0.4 dex higher than the average value $\log(\text{C}/\text{O})$ of ~ -0.75 for low-metallicity SFGs (e.g. Izotov et al. 2023a). Using Cloudy

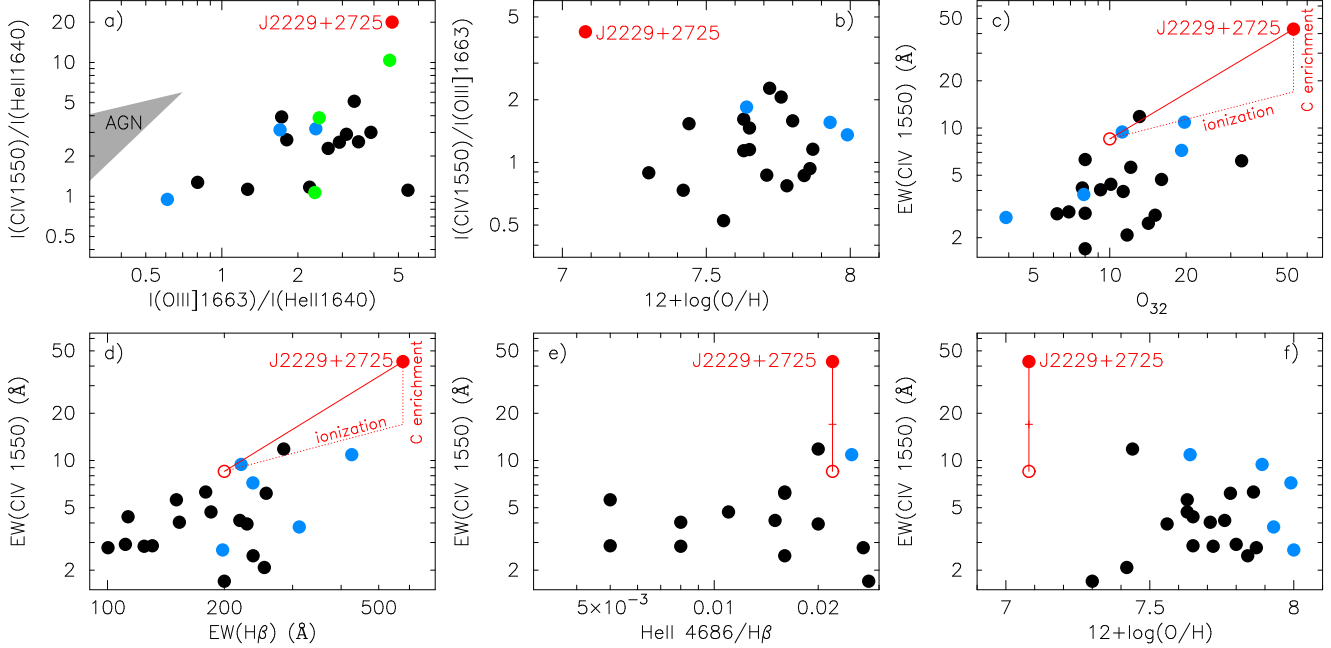


Figure 3. (a) Diagnostic diagram $I(\text{C IV } \lambda 1550)/I(\text{He II } \lambda 1640) - I(\text{O III] } \lambda 1663)/I(\text{He II } \lambda 1640)$. The location of AGN (Tang et al. 2021) is shown by the shaded grey region and labelled. (b) The relation between C IV $\lambda 1550/\text{O III] } \lambda 1663$ flux ratio and oxygen abundance. (c) - (f) Relations between the equivalent widths $\text{EW}(\text{C IV } \lambda 1550)$ and (c) the O_{32} ratios, (d) the equivalent widths $\text{EW}(\text{H}\beta)$ of the $\text{H}\beta$ emission line, (e) the $\text{He II } \lambda 4686/\text{H}\beta$ flux ratio, and (f) the oxygen abundances $12+\log(\text{O}/\text{H})$. In all panels, J2229+2725 is shown by a red filled circle, low-redshift ($z < 0.1$) galaxies from Berg et al. (2016, 2019), Senchyna et al. (2019), Wofford et al. (2021) by black circles and $z \sim 0.3$ LyC leaking galaxies (Schaerer et al. 2022) by blue circles. High-redshift galaxies by Vanzella et al. (2016, 2017, 2020) in (a) are represented by green filled circles. Red open circles in (c) - (f) show the tentative location of J2229+2725 if it would have typical characteristics of the galaxies from the comparison sample, i.e. $\log(\text{C}/\text{O}) = -0.75$, $\text{O}_{32} \sim 10$ and $\text{EW}(\text{H}\beta) \sim 200\text{\AA}$.

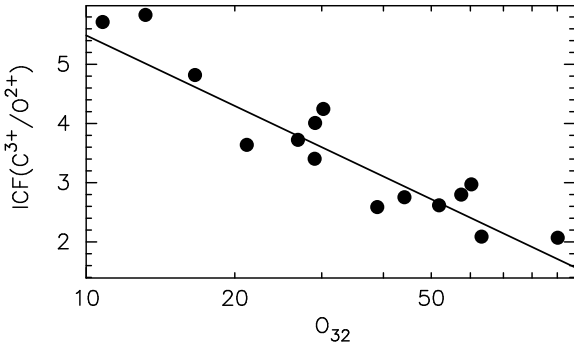


Figure 4. Relation between the ionization correction factor $\text{ICF}(\text{C}^{3+}/\text{O}^{2+})$ and the O_{32} ratio for $\text{O}_{32} \geq 10$ shown by circles and obtained by Izotov et al. (2023a) using the Cloudy code of Ferland et al. (2013). The maximum likelihood regression to the data (Eq. 2) is shown by a solid line.

models, we can estimate the fractions of C^{2+} and C^{3+} in the H II region of J2229+2725. We find that the fraction of C^{2+} in models, predicting $\text{O}_{32} \sim 50 - 60$, is higher by a factor of ~ 1.5 . Then $\log(\text{C}/\text{O}) \sim \log[(\text{C}^{2+} + \text{C}^{3+})/\text{O}^{2+}] = \log(\text{C}^{3+}/\text{O}^{2+}) + 0.4 = -0.76 + 0.4 = -0.36$, or roughly similar to -0.38 derived from $\log(\text{C}^{3+}/\text{O}^{2+})$.

However, the O_{32} ratio can be smaller, because of the decrease of the O^{+} zone by a factor of ~ 1.35 . This results in $\text{O}_{32} \sim 39$ if the LyC leakage is taken into account. But in this case, $\log(\text{C}/\text{O})$ would be further increased by ~ 0.06 dex because of an increasing ICF (Fig. 4).

Additionally, the equivalent width of the C IV $\lambda 1550$

doublet can also increase due to extreme ionization conditions in J2229+2725. This is demonstrated by the relations $\text{EW}(\text{C IV } \lambda 1550) - \text{O}_{32}$ (Fig. 3c) and $\text{EW}(\text{C IV } \lambda 1550) - \text{EW}(\text{H}\beta)$ (Fig. 3d). In both panels, $\text{EW}(\text{C IV } \lambda 1550)$ increases with increasing O_{32} and $\text{EW}(\text{H}\beta)$, respectively, with J2229+2725 having the highest values. Its extremely high $\text{O}_{32} = 53$ corresponds to very intense ionizing radiation compared to other SFGs. A similar conclusion can be drawn from the equivalent width of the $\text{H}\beta$ emission line which is a characteristic of the starburst age. Its extremely high $\text{EW}(\text{H}\beta) = 577\text{\AA}$ indicates a very young age of $\sim 1 - 3$ Myr (Leitherer et al. 1999) for the starburst in J2229+2725. Thus, the top location of J2229+2725 in both relations leads us to conclude that it is the more intense ionizing radiation in this galaxy that is responsible for its higher $\text{EW}(\text{C IV } \lambda 1550)$.

Where would J2229+2725 be located in Fig. 3c and 3d if its characteristics are similar to those in galaxies from the comparison sample, i.e. $\log(\text{C}/\text{O}) = -0.75$, $\text{O}_{32} \sim 10$ and $\text{EW}(\text{H}\beta) \sim 200\text{\AA}$? In this case, $\text{EW}(\text{C IV } \lambda 1550)$ should decrease by a factor of ~ 2.5 due to the correction for the carbon overabundance. Furthermore, the ionization correction factor $\text{ICF}(\text{C}^{3+}/\text{O}^{2+})$ at $\text{O}_{32} \sim 10$, with less intense ionizing radiation, is a factor of ~ 2 higher than the one at the observed value $\text{O}_{32} = 53$ (Fig. 4). This means that the fraction of carbon in the C^{3+} form at a fixed C/O abundance ratio would be lower by the same factor whereas the fraction of oxygen in the O^{2+} form at $\text{O}_{32} \geq 10$ remains nearly constant. Thus, $\text{EW}(\text{C IV } \lambda 1550)$ would be reduced by a factor of ~ 5 due to both effects, attaining a value of

$\sim 8\text{\AA}$, typical of the SFGs from the comparison sample. The reduced value is shown by a red open circle in Fig 3 c-f.

The ionizing radiation may also be harder at low metallicities. However, no correlation is found between the He II $\lambda 4686/H\beta$ flux ratio and EW(C IV $\lambda 1550$) (Fig. 3e) for galaxies from the comparison sample. The galaxy J2229+2725 is off this distribution, but correcting EW(C IV $\lambda 1550$) for enhanced carbon abundance and ionization conditions would move it to the region occupied by other galaxies. Furthermore, the He II $\lambda 4686/H\beta$ flux ratio in this galaxy is in the range of the values observed in galaxies from the comparison sample. Similarly, no correlation between $12+\log(O/H)$ and EW(C IV $\lambda 1550$) is found for galaxies from the comparison sample (blue and black symbols in Fig. 3f). Again, the galaxy J2229+2725 is off this distribution, being the most-metal poor galaxy with an unusually high EW(C IV $\lambda 1550$). After its correction for the two mentioned above effects, we find no correlation, indicating that the ionizing radiation in J2229+2725 with very low metallicity is likely not harder than in other galaxies.

If confirmed by other carbon abundance determinations, e.g. using the C III] $\lambda 1909$ emission line, the origin of the enhanced C/O abundance ratio in J2229+2725 remains to be explained. On the other hand, the N/O abundance ratio is normal for its low metallicity (Izotov et al. 2021a).

4 CONCLUSIONS

We present *Hubble Space Telescope* (HST)/Cosmic Origins Spectrograph (COS) spectrophotometric observations of the compact star-forming galaxy (SFG) J2229+2725. This galaxy possesses extraordinary properties, as derived from earlier optical observations. In particular, it is characterized by a very low oxygen abundance $12 + \log(O/H) = 7.085$, an extremely high O_{32} ratio of 53 and an extremely high equivalent width $EW(H\beta) = 577\text{\AA}$.

We find the properties of this galaxy in the UV to be no less unusual. We discover an extremely strong nebular C IV $\lambda 1550$ doublet in emission with an equivalent width of 43\AA . This is several times higher than in other low- z star-forming galaxies with detected C IV $\lambda 1550$ nebular emission. The detection of such a strong line, together with some other extreme properties of J2229+2725, makes this galaxy an excellent marker, allowing to enlarge the range of characteristics which SFGs at low- and high-redshifts may possess.

We also find that the ionizing radiation in J2229+2725 is stellar in origin. We show that its high EW(C IV $\lambda 1550$) can be explained by a high C/O abundance ratio, ~ 2.5 times higher than the average value for low-metallicity SFGs, and by extreme ionization conditions, characterized by a high O_{32} ratio. These ionization conditions further push EW(C IV $\lambda 1550$) up by a factor of ~ 2 .

Because of its very low metallicity and stellar mass and exceptionally high star-formation activity, J2229+2725 is likely among the best local analogues of star-forming dwarf galaxies in the early universe. The results presented here will thus help to shed light on studies of high-redshift dwarf star-forming galaxies thought to be main source of the reionization of the Universe.

ACKNOWLEDGEMENTS

These results are based on observations made with the NASA/ESA *Hubble Space Telescope*, obtained from the data archive at the Space Telescope Science Institute. STScI is operated by the Association of Universities for Research in Astronomy, Inc. under National Aeronautics and Space Administration (NASA) contract NAS 5-26555. T.X.T. was supported by NASA through grant number HST-GO-17100.002-A from the Space Telescope Science Institute. Y.I.I. and N.G.G. acknowledge support from the National Academy of Sciences of Ukraine by its project No. 0123U102248 “Properties of the matter at high energies and in galaxies during the epoch of the reionization of the Universe” and from the Simons Foundation.

DATA AVAILABILITY

The data underlying this article will be shared on reasonable request to the corresponding author.

REFERENCES

- Aller L. H., 1984, *Physics of Thermal Gaseous Nebulae* (Dordrecht: Reidel)
- Atek H. et al., 2023, preprint arXiv:2308.08540
- Berg D. A., Skillman E. D., Henry R. B. C., Erb D. K., Carigi L., 2016, *ApJ*, 827, 126
- Berg D. A., Erb D. K., Auger M. W., Pettini M., Brammer G. B., 2018, *ApJ*, 859, 164
- Berg D. A., Erb D. K., Henry R. B. C., Skillman E. D., McQuinn K. B. W., 2019, *ApJ*, 874, 93
- Cardelli J. A., Clayton G. C., Mathis J. S., 1989, *ApJ*, 345, 245
- Eldridge J. J., Stanway E. R., Xiao L., McClelland L. A. S., Taylor G., Ng M., Greis S. M. L., Bray J. C., 2017, *PASA*, 34, 58
- Ferland G. J. et al., 2013, *Revista Mexicana de Astronomia y Astrofisica*, 49, 137
- Flury S. R. et al. 2022, *ApJ*, 930, 126
- Hirschauer A. S. et al., 2016, *ApJ*, 822, 108
- Hsyu T., Cooke R. J., Prochaska J. X., Bolte M., 2017, *ApJ*, 845, L22
- Hsyu T., Cooke R. J., Prochaska J. X., Bolte M., 2017, *ApJ*, 863, 134
- Izotov Y. I., Orlitová I., Schaerer D., Thuan T. X., Verhamme A., Guseva N. G., Worseck G., 2016a, *Nature*, 529, 178
- Izotov Y. I., Schaerer D., Thuan, T. X., Worseck G., Guseva N. G., Orlitová I., Verhamme A., 2016b, *MNRAS*, 461, 3683
- Izotov Y. I., Thuan T. X., Guseva N. G., Liss S. E., 2018a, *MNRAS*, 473, 1956
- Izotov Y. I., Schaerer D., Worseck G., Guseva N. G., Thuan, T. X., Verhamme A., Orlitová I., Fricke K. J., 2018b, *MNRAS*, 474, 4514
- Izotov Y. I., Worseck G., Schaerer D., Guseva N. G., Thuan, T. X., Fricke K. J., Verhamme A., Orlitová I., 2018c, *MNRAS*, 478, 4851
- Izotov Y. I., Thuan T. X., Guseva N. G., 2019a, *MNRAS*, 483, 5491

- Izotov Y. I., Thuan T. X., Guseva N. G., 2021a, MNRAS, 504, 3996
- Izotov Y. I., Worseck G., Schaerer D., Guseva N. G., Chisholm J., Thuan T. X., Fricke K. J., Verhamme A. 2021b, MNRAS, 503, 1734
- Izotov Y. I., Chisholm J., Worseck G., Guseva N. G., Schaerer D., Prochaska J. X. 2022, MNRAS, 515, 2864
- Izotov Y. I., Schaerer D., Worseck G., Berg D., Chisholm J., Ravindranath S., Thuan T. X., 2023a, MNRAS, 522, 1228
- Izotov Y. I., Thuan T. X., Guseva N. G., Schaerer D., Worseck G., Verhamme A. 2024, MNRAS, 527, 281
- Kannan R., Garaldi E., Smith A., Pakmor R., Springel V., Vogelsberger M., Hernquist L., MNRAS, 511, 4005
- Katz H. et al., 2021, MNRAS, 507, 1254
- Kojima T. et al., 2020, ApJ, 898, 142
- Leitherer C. et al., 1999, ApJS, 123, 3
- Mascia S. et al., 2023, A&A, 674, 221
- Pérez-Montero E., Amorín R., 2017, MNRAS, 467, 1287
- Rosdahl J. et al., 2018, MNRAS, 479, 994
- Schaerer D. et al., 2022, A&A, 658, L11
- Senchyna P., Stark D. P., 2019, MNRAS, 484, 1270
- Senchyna P., Stark D. P., Chevallard J., Charlot S., Jones T., Vidal-García A., 2017, MNRAS, 472, 2608
- Senchyna P. et al., 2019, MNRAS, 488, 3492
- Senchyna P. et al., 2022, ApJ, 930, 105
- Stark D. P. et al., 2015, MNRAS, 454, 1393
- Tang M., Stark D. P., Chevallard J., Charlot S., Endsley R., Congiu E., 2021, MNRAS, 503, 4105
- Vanzella E. et al., 2016, ApJ, 821, L27
- Vanzella E. et al., 2017, ApJ, 842, 47
- Vanzella E. et al., 2020, MNRAS, 491, 1093
- Wofford A., Vidal-García A., Feltre A., Chevallard J., Charlot S., Stark D. P., Herenz E. C., Hayes M., 2021, MNRAS, 500, 2908

This paper has been typeset from a \LaTeX file prepared by the author.

